Expo Health (2016) 8:389–400
DOI 10.1007/s12403-016-0209-7

ORIGINAL PAPER

Enrichment and Sources of Nitrogen in Groundwater in the Turpan-Hami Area, Northwestern China

Wanjun Jiang[1,2,3] · Guangcai Wang[1,2,3] · Yizhi Sheng[1,2,3] · Dan Zhao[1,2,3] · Chenglong Liu[4] · Yonghai Guo[5]

Received: 1 January 2016 / Accepted: 24 April 2016 / Published online: 9 May 2016

Abstract High contents of nitrogen in groundwater were found in the Turpan-Hami area, Xinjiang, China, whereas the enrichment characteristics and sources of nitrogen were poorly understood. In this study, totally 19 groups of groundwater samples were collected in the Turpan-Hami area for chemistry and isotope analysis. Combining with the hydrochemical, hydrogen, oxygen, and nitrogen stable isotopes data, the distribution and sources of nitrogen of groundwater in the Turpan-Hami area were analyzed. The results showed that the groundwater mainly originated from the atmospheric precipitation, and the evaporation was the dominant mode for groundwater discharge in Turpan-Hami area. The concentration of nitrate (NO_3^-–N) in groundwater varies from 23.29 to 1819.49 mg/L. Obvious enrichment trend of nitrogen was observed along the groundwater flow direction. The increase of nitrate, nitrite, and ammonia concentrations were consistent with that of TDS in the area. The concentrations of nitrogen species were dominated by the strong evaporation rather than human activity except for one sample. The δ^{15}N-NO_3^- in groundwater ranges from −0.6 to +31 ‰, and mostly in a range of +4.1 to +19.3 ‰. The δ^{18}O–NO_3^- ranges from +16.3 to +37.4 ‰. The result indicated that nitrate in groundwater was mainly derived from atmospheric precipitation, and the conversion of nitrate, nitrite, and ammonia in groundwater was not active in the area.

Keywords Hydrochemical characteristics · Stable nitrogen and oxygen isotopes · Nitrate, nitrite, and ammonia · Atmospheric precipitation · Turpan-Hami area

Introduction

Groundwater is an essential part of water resources for human survival and economic development in many regions over the world (Li et al. 2015). It is especially valuable in arid regions where there is only limited availability of precipitation and surface water resources (Li et al. 2016). Groundwater quality which relates closely to human health and economic development has become as important as its quantity due to the demand for safe water (Li et al. 2014). Nowadays, groundwater pollution has been reported in many areas around the world. The major contaminants include heavy metals (Hejabi et al. 2011), nitrate (Mahvi et al. 2005), etc.

In twentieth century, the generally high concentration of NO_3^- in groundwater was found in many arid areas all over the world (Marret et al. 1990; Faillat and Rambaud 1991; Barnes et al. 1992). Excess levels of nitrate in groundwater can cause methemoglobin disease and cancer, posing an extreme threat to human health especially to the development of children's health (Kendall and Aravena 2000; Knobeloch et al. 2000; Weyer et al. 2001). As an

✉ Guangcai Wang
wanggc@pku.edu.cn

1 School of Water Resources and Environment, China University of Geosciences, Beijing 100083, China

2 State Key Laboratory of Biogeology and Environmental Geology, China University of Geosciences, Beijing 100083, China

3 MOE Key Laboratory of Groundwater Circulation and Evolution, China University of Geosciences, Beijing 100083, China

4 Institute of Geology, China Earthquake Administration, Beijing 100029, China

5 Beijing Research Institute of Uranium Geology, Beijing 100029, China

important material in the nitrogen cycle and widely participating in physical, chemical, and biological reactions in groundwater, nitrate has attracted extensive attention (Canter 1997; Galloway et al. 2003).

Arid and semi-arid area, which is prone to high concentration of nitrate under the condition of extreme drought, can serve as the main storage area for nitrogen (Walvoord et al. 2003; Smith et al. 2000; Schaeffer et al. 2003). Turpan-Hami area, or Tu-Ha area, located in the northwest arid areas of China, which is an important part of the Silk Road economic belt (Li et al. 2015), is the largest nitrate accumulation area in China (Qin et al. 2012a, b). Such high concentrations of nitrate in the groundwater can cause serious health risk to local residents. Therefore, it is of scientific and realistic significance to investigate and find out the distributions and sources of nitrate in groundwater for the water resources utilization and management.

In recent years, the nitrogen and oxygen isotopic techniques have been well developed and widely applied to trace and distinguish the source and formation conditions of nitrate (Deng et al. 2007; Wang 1997; Wigand et al. 2007; Lee et al. 2008; Mattern et al. 2011), which can largely avoid the uncertainty of a single isotope tracer. Many studies have shown that the determination of $\delta^{18}O$ and $\delta^{15}N$ in NO_3^- is not only an effective tool to identify the different sources of NO_3^-, but also a useful way for the study of migration and transformation of NO_3^- in the groundwater (Seiler 2005; Widory et al. 2005; Umezawa et al. 2008). Recently, some studies focus on the in-depth research about the source of NO_3^- in groundwater and zone of aeration in Xinjiang and Badain Jaran Desert by using isotopic techniques (Gates and BÖHLKE 2008; Ge et al. 2014; Qin et al. 2012a, b). These studies indicate that the sedimentation of atmospheric aerosol is the main source of NO_3^- in the nitrate deposits in the Tu-Ha basin, Xinjiang (Qin et al. 2008, 2012a, b). However, the scant attention has been paid to the concentration and source of nitrate in groundwater in the Tu-Ha area. In present study, the hydrogeological, isotopic, and hydrogeochemical information were integrated in an attempt to explore the source, migration, and transformation of nitrogen in the groundwater in the Tu-Ha area. The data evaluation methods and results of this study could be useful to the protection and management of groundwater resources in Tu-Ha area and other arid and semi-arid areas.

Study area Description

Natural Geography

The study area, which was divided into two workspaces, Turpan area and Hami area, is located in the Turpan-Hami area, Xinjiang, China. The geographic coordinates are from 41°40′ to 42°40′ N and 90°00′ to 94°00′ E (Fig. 2). In the study area, the topography goes up from northwest to southeast. The peneplain hilly terrain is widely distributed in the south of the study area and the plain terrain covers large areas in the north. South Lake Gobi Desert, Geshun Gobi Desert, Big Depression, and Kumutage Desert are located in the study region. Hami City is 100 km away on the northeast of the study area; Aydingkol Lake and Turpan City are 200 km away to the northwest of the region.

The study area has the typical continental climate, and is one of the regions with most intense continental climate in the world. The earth's surface, where only a small amount of drought-resistant plant and animal could grow, e.g., ephedra, hay, and antelope, is covered with broad gobi gravel. The region lacks rain and has a large difference in temperature between day and night. The annual average temperature is 9.8 °C and the annual rainfall is from 30 to 57.5 mm. The annual average evaporation is from 2245 to 2879 mm, and is much larger than the precipitation in the study region. Due to scarce rainfall, the surface runoff is not developed and the arid desert landscape exists everywhere in the region. Although there is no perennial river, the dry valleys are widely distributed and mostly formed by flood erosion. The river water which distributes in the mountainous area gradually disappears in the gobi after flowing into basin.

Hydrogeology

According to the geological structure, lithology, aquifer and hydrodynamic characteristics, etc., the groundwater in Hami area could be divided into four types: loose sediment pore water, clastic rock cranny pore water, carbonate fissure water, and bedrock fissure water. The area of loose sediment pore water is relatively large and mainly distributed in the intermountain depression and valleys area. The thickness of the loose debris can be up to 7 m. The lithology of clastic rock cranny pore water is mainly tertiary glutenite and mostly exist in the intermountain depression. Carbonate fissure water mainly distributes around Yamansu Iron ore and has a relatively high water content. Bedrock fissure water is the main type of groundwater in the Hami area, and it mainly includes weathering fissure water and structural fissure water. Within the depth of several meters below the surface, weathering fissures develop best and the development degree gradually weakens with the increase of depth. The development depth of rock weathering fissure water in the study area is from 10 to 30 m and only few areas can reach 100 m. Previous studies showed that the groundwater generally flows from southeast to northwest, based on the measurements of water depth in 30 wells in the Hami area (Guo et al. 2014, 2016). Combining the data of the water depth from the previous and present studies, the groundwater flow directions were roughly drawn (Fig. 1).

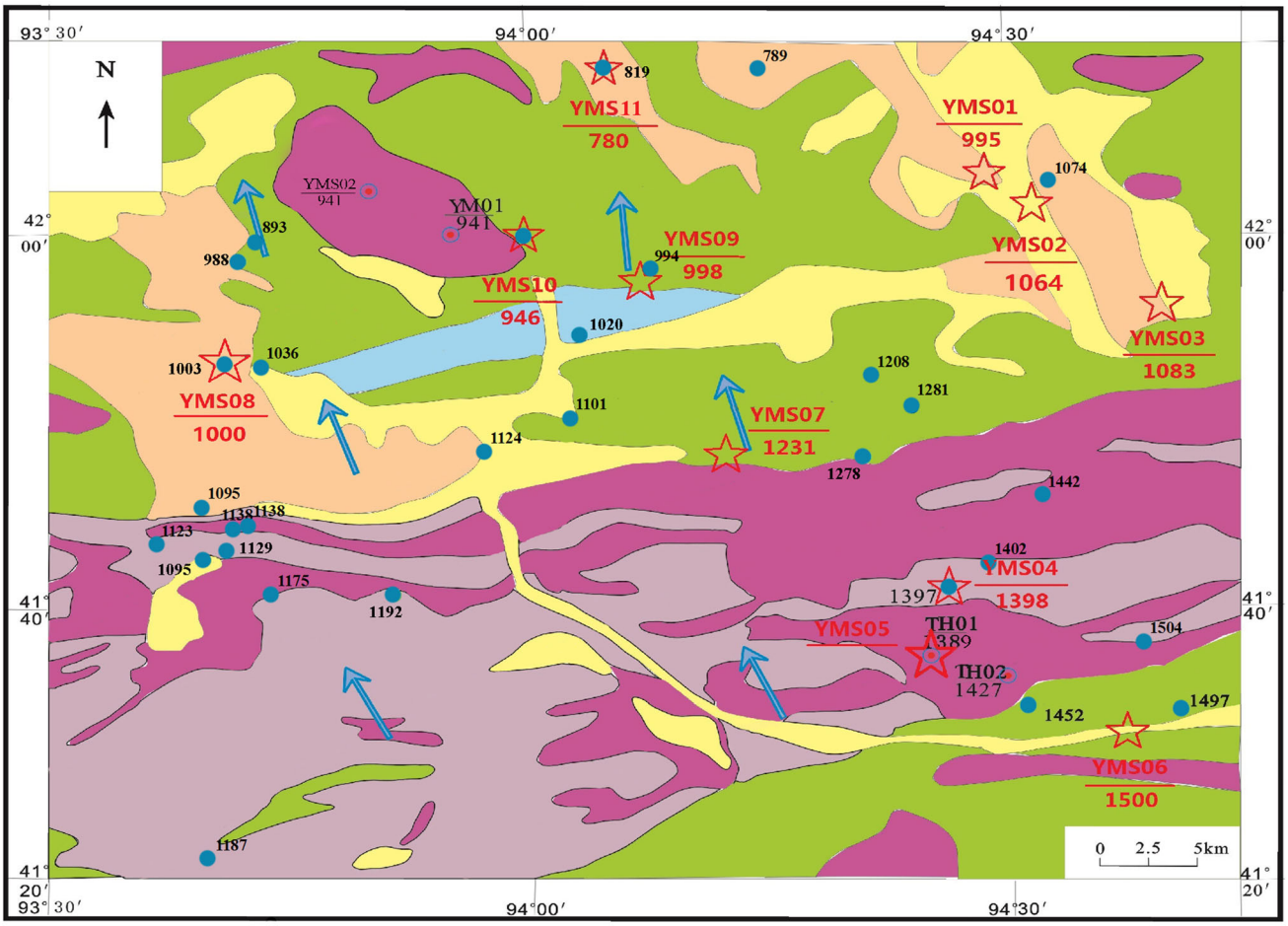

Legend

1. Groundwater type
   - Loose rock pore water
   - Clastic rock pore fissure water
   - Carbonate rock fissure water
   - Clastic rock fissure water
   - Igneous rock fissure water
   - Metamorphic rock fissure water
2. Hydrogeological point
   - Hydrogeological investigation points (Water level "m")
   - Drills
3. Others
   - Groundwater type boundaries
   - Direction of groundwater flow
   - Sampling points — Number / Water level (m)

Fig. 1 The hydrogeological map of Hami area

Groundwater Sampling and Analysis

Sampling Point Layout

In the study area, totally 19 groups of samples were collected. The workspace in the southeast of Turpan basin is located in south of the Kumutage desert and north of the Kuruketag mountain. 8 groups of groundwater samples were collected in this workspace and the sample numbers were labeled from SS12 to SS19. There were 2 groups of spring water, 4 groups of shallow groundwater, and 2 groups of deep groundwater. The other workspace is located in the southeast of the Hami basin, as a typical study area. This area is located in the southeast of South Lake Gobi Desert and the south of Hami city. 11 groups of groundwater samples in this workspace were collected and

the sample numbers were labeled from YMS01 to YMS11. Among them there were 3 groups of spring water, 7 groups of shallow groundwater, and 1 group of deep groundwater. We analyzed the concentrations of major ions, including Cl^-, SO_4^{2-}, CO_3^{2-}, HCO_3^-, Na^+, K^+, Mg^{2+}, and Ca^{2+}, for all the samples collected in the Tu-Ha area. The hydrogen and oxygen stable isotopes of 15 groundwater samples were measured, and nitrogen and oxygen stable isotopes of nitrate for 19 groups of samples were tested. The concentrations of NO_3^-–N, NO_2^-–N and NH_4^+–N for 15 groups of samples were measured in the study area (Fig. 2).

Isotopes and Hydrochemistry Analysis

The major ions of groundwater in this study were analyzed by ion chromatography (Anionic chromatography DX-120 and Cationic chromatography ICS900) and the data were assessed according to national standard of the People's Republic of China: Quality standard for groundwater (GB/T 14848-93). A charge balance check showed that the error is <10 % for all samples except for one sample YMS08. The error rate of sample YMS08 is as high as 86 %. Due to high concentrations of Na^+ that exceeded the detection limitation of instrument, Na^+ was not measured in the SS16 sample. Therefore, the ions

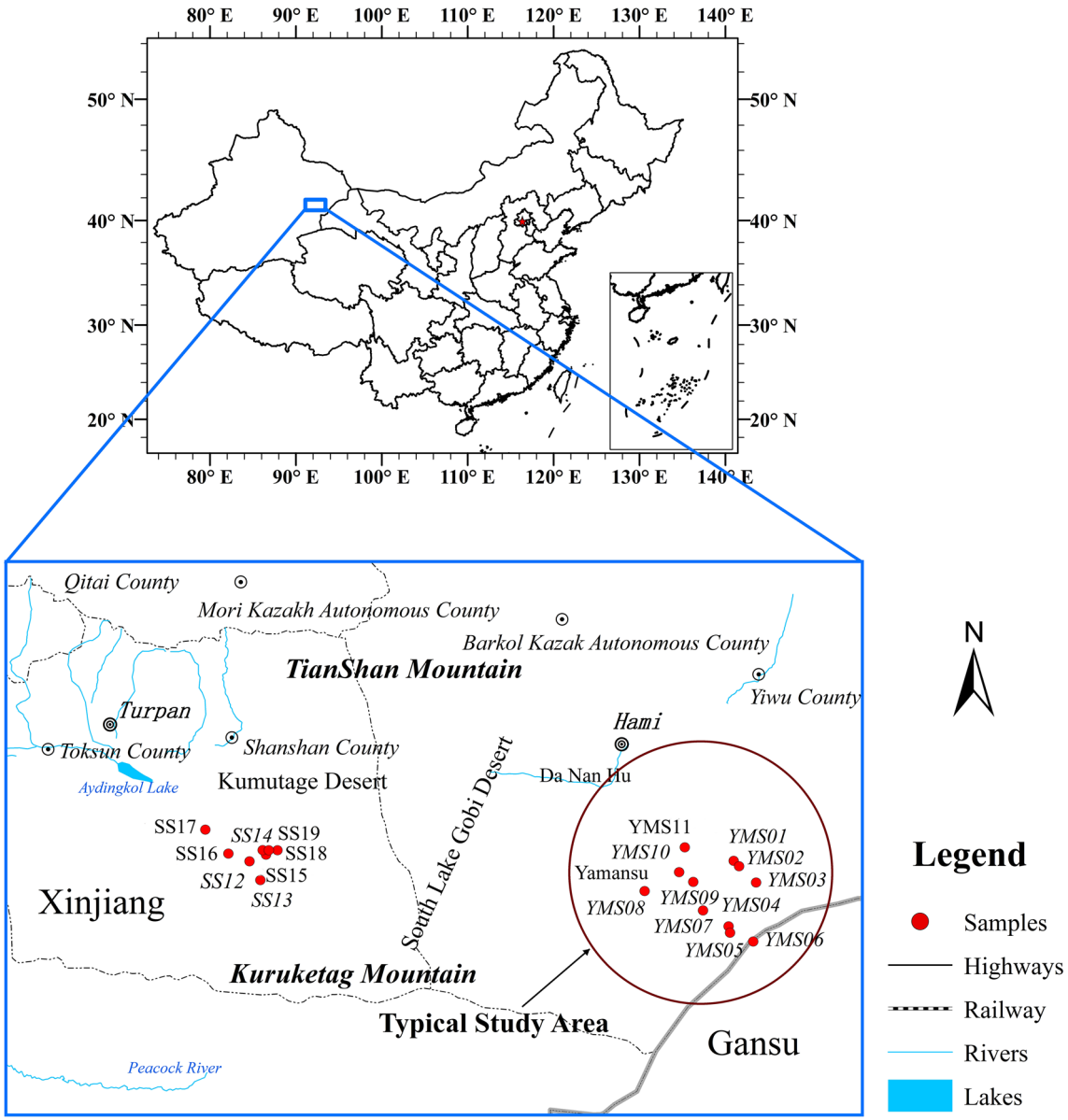

Fig. 2 Locations of the groundwater samples

Table 1 Correlation coefficient (R) matrix of groundwater chemical composition in Tu-Ha area

	TDS	Cl^-	SO_4^{2-}	Na^+	Mg^{2+}	Ca^{2+}	NH_4^+–N	NO_2^-–N	NO_3^-–N	Total N	pH
TDS	1.00	0.98**	0.73*	0.90**	0.89**	0.79**	0.91**	0.93**	0.96**	0.98**	0.45
Cl^-		1.00	0.74*	0.82**	0.82**	0.71*	0.91**	0.92**	0.97**	0.98**	0.31
SO_4^{2-}			1.00	0.45	0.37	0.34	0.80**	0.54	0.85**	0.83**	0.23
Na^+				1.00	0.99**	0.91**	0.75*	0.86**	0.78**	0.81**	0.67*
Mg^{2+}					1.00	0.92**	0.72*	0.879**	0.74*	0.78**	0.60
Ca^{2+}						1.00	0.66*	0.73*	0.66*	0.68*	0.56
NH_4^+–N							1.00	0.76*	0.93**	0.93**	0.34
NO_2^-–N								1.00	0.82**	0.86**	0.43
NO_3^-–N									1.00	0.99**	0.33
Total N										1.00	0.35
pH											1.00

** Significant correlation at 0.01 level (double side), * Significant correlation at 0.05 level (double side)

data of groundwater were not convincible for YMS08 and SS16 samples in this study. Liquid water isotope analyzer was used for the analysis of hydrogen and oxygen isotopes. The NO_3^-–N, NO_2^-–N, and NH_4^+–N concentrations were determined by spectrophotometer according to "Standard methods for the examination of water and waste water" (State Environmental Protection Administration of China, 2002). The nitrogen and oxygen stable isotopes in NO_3^- of groundwater were analyzed by isotope mass spectrometer (MAT 253) in the Institute of geographical science and resources, Chinese academy of sciences (the precision of $\delta^{15}N$–NO_3 and $\delta^{18}O$–NO_3 is ±0.3 ‰).

Data Analysis

By using the method of the relational graph of hydrogen and oxygen stable isotopes in groundwater, obtained by Origin 9.0 software (Seifert 2014), the recharge source and discharge of groundwater in Tu-Ha area were analyzed. The chemical composition of groundwater was studied by using the Piper diagram that was drawn by AqQA software (Geoffrey et al. 2004). The correlation of groundwater chemical characteristics was calculated by SPSS20 software and the ion contour maps of NO_3^-–N, NO_2^-–N, NH_4^+–N, and TDS in the study area were drown by Surfer11 (Hasanah et al. 2013). Combining with the correlation and the ion contour map, the characteristics of distribution and the circulation of nitrogen in groundwater were discussed. The source characteristics of nitrate in groundwater in the study area were identified by the diagram of $\delta^{15}N$ and $\delta^{18}O$ in NO_3^- (Origin 9.0).

Results And Discussion

A statistically correlation analysis was conducted to assess the correlation between the major ions. From the formation of correlation matrix, the correlation coefficient of each groundwater component can be clearly seen, and the NO_3^-–N, NO_2^-–N, and NH_4^+–N sources can be inferred from the value of the correlation coefficient among the components. According to the correlation coefficient matrix of groundwater chemical composition (Table 1), NO_3^-–N, NO_2^-–N, NH_4^+–N, and total nitrogen have higher correlation coefficient with each other and also have a higher correlation coefficient with the major ions compositions (e.g., Cl^-, SO_4^{2-}, Na^+). Especially, the correlation coefficient is over 0.91 among NO_3^-–N, NO_2^-–N, NH_4^+-N, and Cl^-, TDS. The concentrations of NO_3^-–N, NO_2^-–N, NH_4^+–N, and total nitrogen increase with the rising of TDS and the change of NO_3^-–N, NO_2^-–N, NH_4^+–N is almost the same with the major ions compositions of groundwater. Meanwhile, the correlation coefficient among NO_3^-–N, NO_2^-–N, NH_4^+–N and pH is very low. It indicated that the formation of high level nitrogen in groundwater, which is mainly affected by strong evaporation, is almost the same as that of high concentration of Cl^-, Na^+, and SO_4^{2-}.

Distribution Characteristics of Nitrogen

The main hydrochemical components of groundwater in Tu-Ha area are Cl^-, Na^+, and SO_4^{2-}, but it can be illustrated that the contents of NO_3^-–N, NO_2^-–N, and NH_4^+–N are very high. In the groundwater samples of Tu-Ha area, the concentrations of NO_3^--N vary from 23.29 to 1819.49 mg/L, NO_2^-–N vary from 0.006 to 102.25 mg/L and NH_4^+–N vary from 0.02 to 2.53 mg/L. However, except for sample SS13, the hydrochemical types of the rest samples are invariant with the changes of NO_3^-–N, NO_2^-–N, and NH_4^+-N concentrations in study area. According to the national standard of "the People's Republic of China: Quality standard for groundwater"

(GB/T 14848-93), the NO_3^-–N concentration in all samples exceeds the standard of class III, equivalent to the drinking water standard (class III:5 mg/L<NO_3^-–N ≤ 20 mg/L, class IV:20 mg/L<NO_3^-–N ≤ 30 mg/L, class V:NO_3^-–N>30 mg/L). Meanwhile, YMS02, YMS03, and YMS04 belong to class V, and the rest 12 groups of samples belong to class V. The NO_3^-–N concentration of SS13 sample is the highest, being as much as 1819.49 mg/L. The site of SS13 is located in the local large granite mining area, and human activities may have potential influences on the groundwater flow and water quality, leading to the unusually high concentration of NO_3^-–N in groundwater.

In the typical study area (Hami area), covering approximately 3700 km^2, the flow direction of groundwater is roughly from southeast to northwest. TDS constantly increases from the southeast to the northwest along the groundwater flow direction. Meanwhile, the concentrations of NO_3^-–N, NO_2^-–N, and NH_4^+–N also increase from southeast to northwest (Fig. 3). The enrichment of nitrate, nitrite, and ammonia has similar trend with TDS and all have the similar trends of rising along the groundwater flow direction.

The Isotopic and Chemical Characteristics of Groundwater

According to the diagram showing the relationship between hydrogen and oxygen stable isotopes of groundwater (δD and $\delta^{18}O$), we discussed the hydrogeochemical formation of groundwater. Compared with the Global Meteoric Water Line (GMWL) (Fig. 4), we found that all the points of groundwater samples lie in the lower right of the GMWL and are far away from the line. A linear

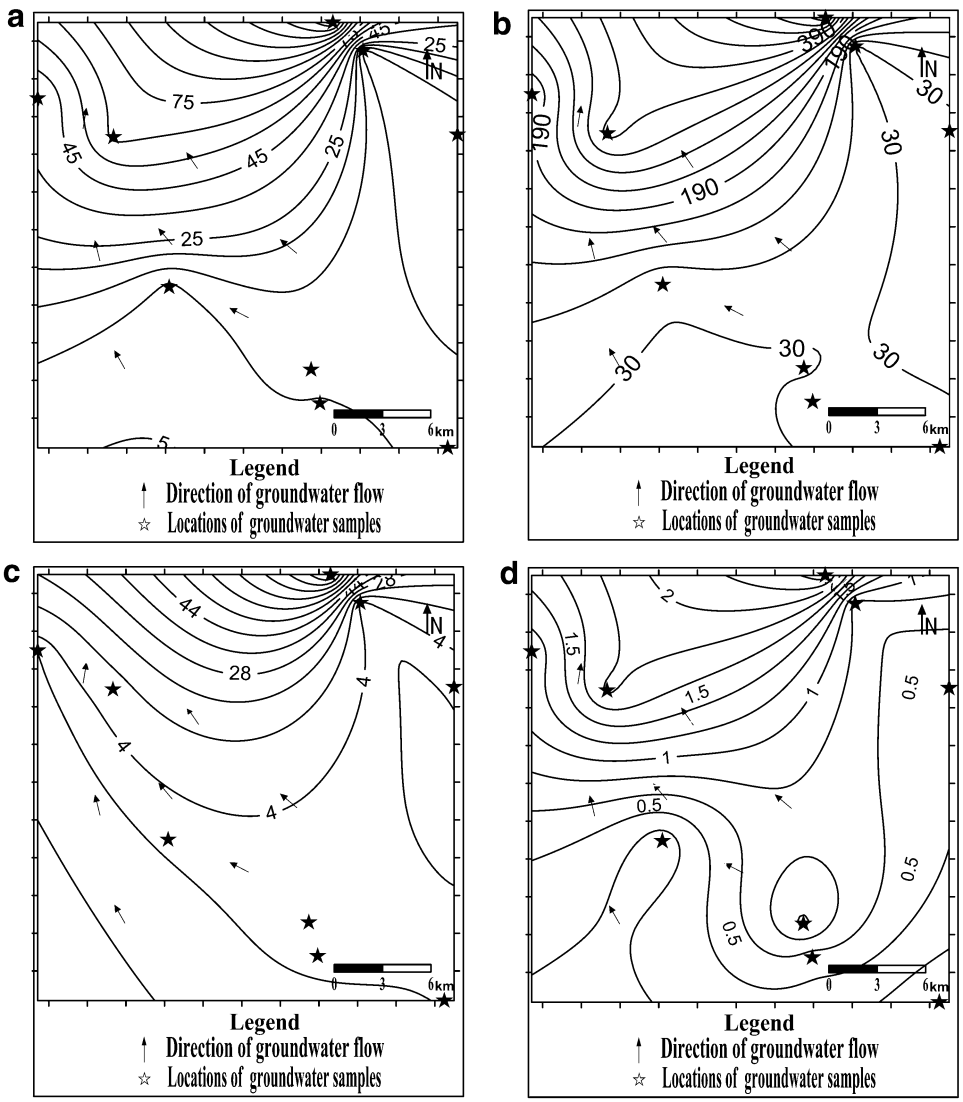

Fig. 3 Contour graph of Nitrogen and TDS in the Hami area: **a** Contour graph of TDS (g/L); **b** Contour graph of NO_3^-–N(mg/L); **c** Contour graph of NO_2^-–N(mg/L); **d** Contour graph of NH_4^+-N(mg/L)

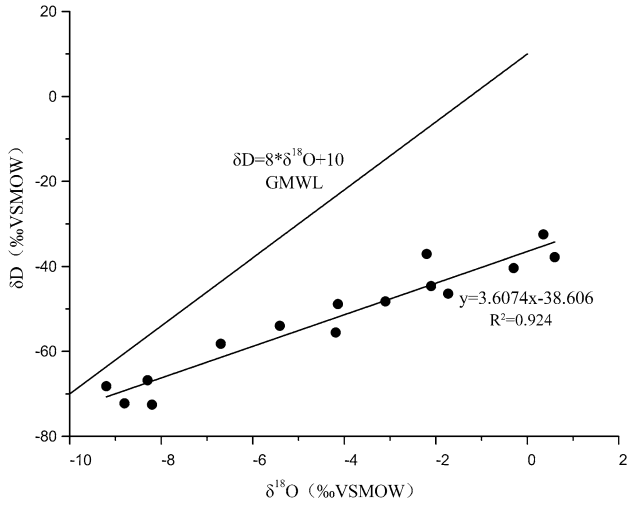

Fig. 4 Plot of δD versus $\delta^{18}O$ in Tu-Ha area

regression line was fitted using the data of δD and $\delta^{18}O$ of all the samples, which is approximately $\delta D = 3.6\delta^{18}O$–38.6 with $R^2 = 0.924$, representing an evaporation line. The concept of evaporation line comes from the fact that the evaporation will cause waters deviating from the GMWL and distributing along the lines with the slopes less than 8 (usually between 3.5 and 6 or from 4 to 6) (Friedman et al. 1962). The relatively enrichment of heavy isotopes in the groundwater could be caused by non-equilibrium evaporation process (Clark and Fritz 1997). The result indicated that the main recharge source of groundwater is from atmospheric precipitation and the groundwater in study area has experienced strong evaporation and concentration effects.

It can be seen from the Piper diagram of groundwater chemistry (Fig. 5) that the main chemical types of groundwater are Cl·SO_4–Na and Cl–Na (except SS13), confirming that groundwater chemistry is mainly influenced by strong evaporation in the study area. In arid and semi-arid area, the groundwater levels are relatively shallow and evaporation becomes the main discharge of groundwater. Under the effect of evaporation, the moisture of groundwater is constantly evaporated and salts with lower solubility precipitates with the continuation of time. In contrast, the salts with higher solubility would stay in the water (e.g., NaCl), and become the main components of groundwater with high TDS. As shown in Table 2, among the shallow groundwater, the chemical type of YMS01, YMS08, YMS09, and SS12 is Cl–Na, YMS02, YMS03, YMS04, and YMS07 is Cl·SO_4–Na water. For the spring water, the type of YMS06, YMS08, and SS18 is also Cl·SO_4–Na and YMS10 is Cl–Na water. In the deep groundwater, the type of YMS05 is SO_4·Cl–Na, SS13 is NO_3–Na and SS14 is Cl·SO_4–Na water. Meanwhile, the type of groundwater chemistry is gradually from Cl·SO_4–Na to Cl–Na along the direction of groundwater flow in the

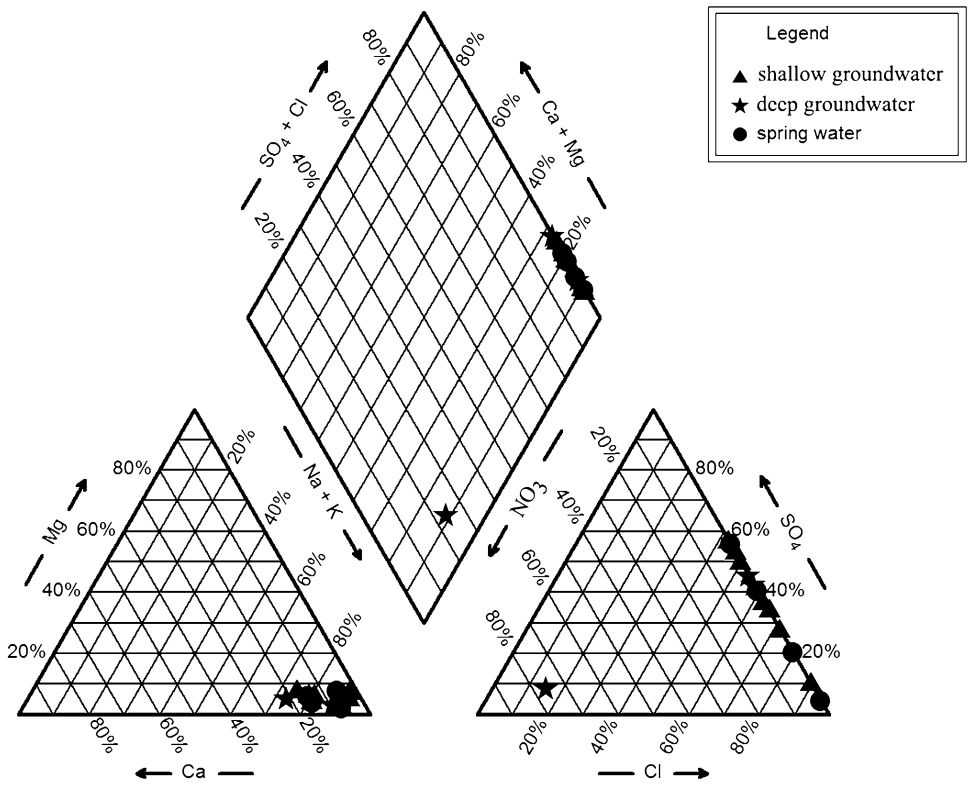

Fig. 5 Piper graph of water chemistry in Tu-Ha area

Table 2 Statistics of major ions and water depths, Ion concentration unit(mg/L)

Sample	TDS(g/L)	Cl^-	SO_4^{2-}	CO_3^{2-}	HCO_3^-	Na^+	K^+	Mg^{2+}	Ca^{2+}	Water depth (m)
YMS01	144.2	80792.0	11981.0	21.1	107.6	47851.0	301.3	1889.4	1284.3	2.0
YMS02	7.6	3298.0	2282.0	0.0	326.4	1424.7	22.7	55.0	200.0	0.6
YMS03	6.9	1657.6	2935.8	0.0	147.0	1677.5	23.1	86.4	336.8	1.6
YMS04	14.3	3810.0	5802.1	12.3	39.4	3797.7	50.0	147.7	611.3	1.2
YMS05	9.3	3035.6	3040.5	0.0	68.1	2367.1	46.9	86.9	615.3	Unknown
YMS06	11.8	2872.7	4922.7	0.0	276.1	3067.4	40.7	125.1	514.7	Spring
YMS07	8.8	2448.8	3291.8	0.0	136.3	2402.3	36.3	60.9	382.7	1.3
YMS09	67.0	27331.0	14016.0	35.2	69.9	23734.1	295.9	663.9	808.6	0.1
YMS10	34.0	17863.0	1155.6	22.9	378.4	12275.8	964.1	592.6	780.0	Spring
SS12	28.8	10535.4	8180.8	14.1	64.6	9125.5	80.7	122.6	634.7	1.2
SS13	10.6	213.6	157.3	0.0	118.3	9074.7	90.6	155.1	742.5	Unknown
SS14	19.1	5908.3	6677.0	0.0	102.2	5700.9	40.2	101.7	552.2	80.0
SS18	34.7	12246.2	11390.0	31.7	46.6	10059.5	80.6	109.8	725.3	Spring

typical research area and the TDS ranges from 4 to 100 g/L (Table 2).

Source Characteristic of Nitrate

Cl^- is widely distributed in various kinds of water body, and it is relatively stable. Due to the stability of Cl^-, it has often been used as atmospheric precipitation inert tracer. The ratio of NO_3^-–N/Cl^- can standardize the influence extent of evapotranspiration and also can be used as a basic index for distinguishing the nitrate sources of atmospheric precipitation from other sources (Gates et al. 2008). According to the previous study in the northwestern region of China, the reference value of NO_3^-–N/Cl^- which could represent the value without human activities is 0.05–0.22 (Ma and Edmunds 2006, Ma et al. 2009; Li 2014; Pan 2014; Huang 2005; Dang et al. 2010). The figure shows that the concentration of NO_3^-–N increases with the rise of concentration of Cl^- (except SS13) (Fig. 6), while the NO_3^-–N/Cl^- remained at a low value ranging from 0.02 to 0.05 (Table 3). And besides SS13, there is high correlation between the source of NO_3–– N and that of Cl^-. The reason for the high NO_3^-–N/Cl^- ratio of SS13 (up to 21.6) is that SS13 is located in the quarry mining area, and large-scale human exploitation activities possibly lead to the increasing content of nitrate. Also it shows that except SS13 the main nitrate sources of groundwater samples in study area is the natural source (atmospheric sedimentation), not the non-natural sources produced by human activities.

On the basis of the eigenvalue of nitrogen stable isotope ($\delta^{15}N$–NO_3^-) and oxygen stable isotope ($\delta^{18}O$–NO_3^-), the source of nitrate can be determined because the isotopes of different nitrate sources have different eigenvalues. In the atmospheric precipitation (dry precipitation and wet precipitation), the eigenvalue of $\delta^{15}N$–NO_3^- ranges from −15 to +15 ‰ and the eigenvalue of $\delta^{18}O$–NO_3^- ranges from +18 to +70 ‰. In the values of inorganic fertilizers, the $\delta^{15}N$–NO_3^- ranges from −4 to +4 ‰ and the $\delta^{18}O$–NO_3^- ranges from 17 to +25 ‰. In mineralization of soil organic matter (microbiological nitrification nitrogen), the $\delta^{15}N$–NO_3^- ranges from +4 to +8 ‰ and the $\delta^{18}O$–NO_3^- ranges from −10 to +10 ‰. In manure or sewage, the $\delta^{15}N$–NO_3^- ranges from +8 to +22 ‰ and the $\delta^{18}O$–NO_3^- ranges from +3 to +8 ‰ (Heaton 1990; Kendall 1998b, 2007; Choi et al. 2003). In 19 groups of the samples in Tu-Ha area, the $\delta^{15}N$–NO_3^- ranges from −0.6 to +31 ‰ and mainly between +4.1 and +19.3 ‰, and the $\delta^{18}O$–NO_3^- ranges from +16.3 to +37.4 ‰. The $\delta^{15}N$–NO_3^- of most

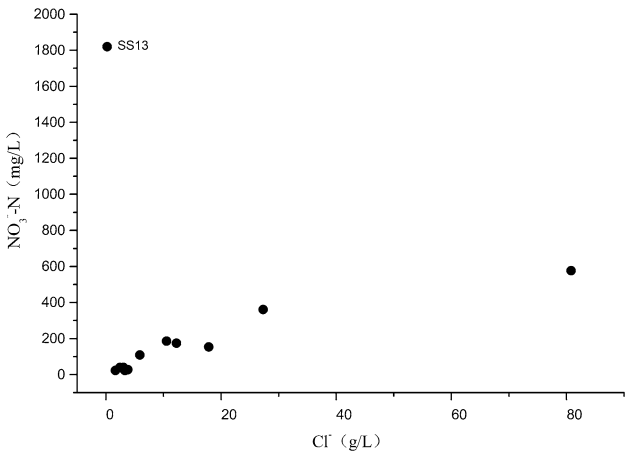

Fig. 6 Plot of NO_3^-–N versus Cl^- in Tu-Ha area

Table 3 NO_3^--N, NO_2^--N, and NH_4^+-N data of groundwater in Tu-Ha area,(mg/L)

Sample	NH_4^+–N	NO_2^-–N	NO_3^-–N	NO_3^-–N/Cl^-
YMS01	2.53	102.25	577.22	0.02
YMS02	0.71	1.37	23.29	0.02
YMS03	0.4	0.74	23.29	0.04
YMS04	1.05	2.04	27.37	0.02
YMS05	0.5	0.74	39.58	0.03
YMS06	0.02	0.11	35.51	0.03
YMS07	0.08	0.88	39.58	0.04
YMS09	1.84	7.97	361.35	0.03
YMS10	1.05	0.006	153.63	0.02
SS12	1.2	0.66	186.21	0.04
SS13	0.34	0.12	1819.49	21.6
SS14	0.46	0.02	108.83	0.05
SS18	1.31	16.85	173.99	0.04

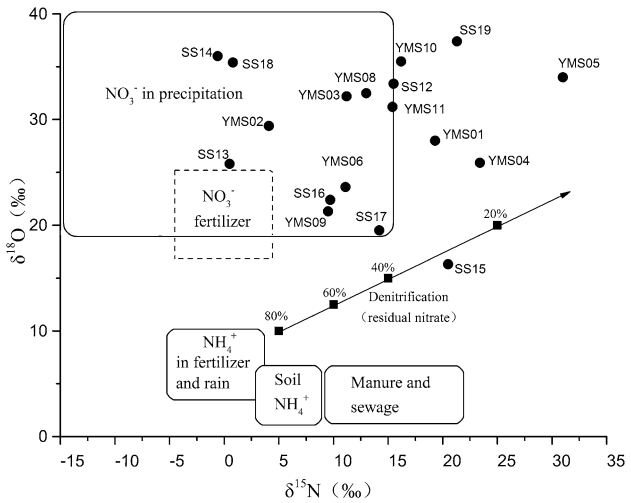

Fig. 7 Plot of $\delta^{15}N$ versus $\delta^{18}O$ in Tu-Ha area (Kendall et al. 1998; Kendall and McDonnell 1998; Kendall and Aravena 2000)

groundwater samples is within the range of atmospheric precipitation as previously shown. Except for SS15, the $\delta^{18}O$–NO_3^- of the rest samples is within the range of atmospheric precipitation. Compared with the previous research which showed that the long sedimentation of atmospheric aerosol is the main source of NO_3^- in the nitrate deposits in Tu-Ha basin (Qin et al. 2008, 2012a, b), we found that the values of $\delta^{15}N$–NO_3^- and $\delta^{18}O$–NO_3^- of groundwater samples are similar to that of the nitrate deposits in Qin's research. According to the previous and the present research, the nitrate in Tu-Ha area is mainly derived from atmospheric precipitation, and local or regional isotope differences in nitrate deposits may be attributed to post-depositional processes, and the difference in aridity and associated microbial activities.

The previous studies have suggested a diagram of $\delta^{15}N$ versus $\delta^{18}O$ to trace the sources of nitrate in water by taking the nitrogen stable isotope as abscissa and the oxygen stable isotope as ordinate (Kendall et al. 1998; Kendall and McDonnell 1998; Kendall and Aravena 2000). Accordingly, the source of nitrate could be more accurately inferred via the diagram of $\delta^{15}N$ and $\delta^{18}O$ in the Tu-Ha area. Most samples but YMS01, YMS04, YMS05, YMS10, and SS19 in the Tu-Ha area are located in the nitrate distribution area caused by atmospheric precipitation (Fig. 7), indicating that the source of nitrate is mainly from atmospheric precipitation. According to the site investigation, there are no human activities and livestock, and wild animals are very scarce around YMS01, YMS04, YMS05, YMS10, and SS19 samples. Meanwhile it can also be proved from the mass-independent fractionation effect of oxygen isotope in the nitrate deposits of Tu-Ha area that the nitrate is produced by atmospheric photochemical reaction (Qin et al. 2008; Li et al. 2010). In the sample of SS15, which is located near the line of denitrification, it suggests that the phenomenon of local denitrification exists.

In the process of denitrification, the concentration of nitrate is low and $\delta^{15}N$–NO_3^- is high because the ^{15}N–NO_3^- becomes abundant in the rest of nitrate after ^{14}N–NO_3^- participates in the reaction. Meanwhile, it also causes the fractionation of oxygen stable isotope in NO_3^- and the enrichment of ^{18}O–NO_3^- in the rest of the nitrate. According to the analysis of the concentration relationship between $\delta^{15}N$, $\delta^{18}O$, and NO_3^-–N, the denitrification can be clearly judged. If $\delta^{15}N$ and $\delta^{18}O$ increase with the decrease of nitrate concentration and a linear relationship presents between $\delta^{15}N$, $\delta^{18}O$, and the rest of ln [NO_3^-–N], denitrification will occur in the aquifer of study area (McKeon et al. 2005; Chen et al. 2006). Therefore, the changes of $\delta^{15}N$–NO_3^- and ^{18}O–NO_3^- could be used as an indicator of denitrification. It shows that the changes of $\delta^{15}N$–NO_3^-, ^{18}O–NO_3^-, and the rest of ln [NO_3^-–N] do not present a linear relationship (Figs. 8, 9), and the $\delta^{15}N$–NO_3^- and ^{18}O–NO_3^- do not increase according to the proportion of 1.3:1 to 2.1:1 (Aravena and Robertson 1998; Böttcher et al. 1990) (Fig. 7). The DO concentrations of groundwater change between 1.82 and 3.73 mg/L, and most of them are higher than 2 mg/L which is not suitable for denitrification. Thus, we can speculate that denitrification does not take place in Tu-Ha area.

When NH_4^+–N transfers to NO_3^-–N through the nitrification in groundwater, 1/3 of oxygen in demand is from atmosphere and the rest 2/3 of oxygen is from the oxygen of nitrification environment (generally refers to the water)(Andersson and Hooper 1983; Hollocher 1984; Mariotti et al. 1981). Therefore, the enrichment degree of ^{18}O in the nitrate can be used to determine whether the

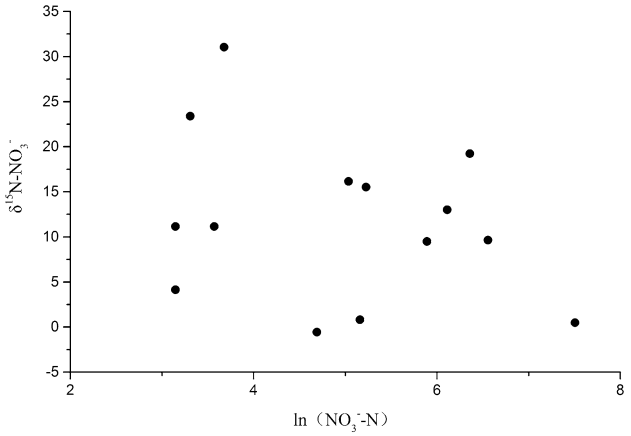

Fig. 8 Plot of $\delta^{15}N$ versus ln [NO_3^-–N]

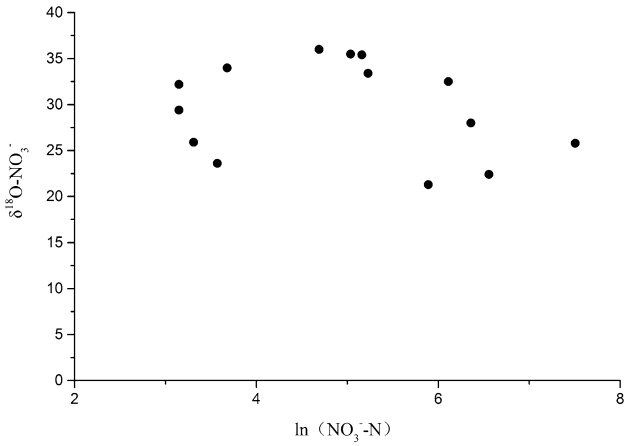

Fig. 9 Plot of $\delta^{18}O$ versus ln [NO_3^-–N]

nitrification happens, because the $\delta^{18}O$ in the nitrate formed by nitrification is closed to the $\delta^{18}O$ in local groundwater. Due to the relative stability of oxygen isotopic composition in the atmosphere, the $\delta^{18}O$ in nitrate formed by nitrification mainly depends on the oxygen isotopic composition of local groundwater (Andersson and Hooper 1983; Mariotti et al. 1981). Therefore, the oxygen isotopic composition in nitrate formed by microbiological nitrification can approximately be calculated using the following equation: $\delta^{18}O\text{–}NO_3^- = 2/3(\delta^{18}O\text{–}H_2O) + 1/3(\delta^{18}O\text{–}O_2)$. The value of $\delta^{18}O\text{-}O_2$ is +24 ‰ (Hollocher 1984; Durka et al. 1994) and the $\delta^{18}O\text{-}H_2O$ of groundwater in study area ranges from −9.2 to +0.6 ‰. The $\delta^{18}O\text{–}NO_3^-$of groundwater in Tu-Ha area calculated by the formula ranges from +1.87 to +8.4 ‰. However, the actual value of $\delta^{18}O\text{–}NO_3^-$ in study area ranges from +16.3 to +37.4 ‰, inconsistent to the calculated values of $\delta^{18}O\text{–}NO_3^-$. Many studies have shown that the optimum pH range of nitration ranges from 6.4 to 7.9 and either higher or lower value of pH will have different influences on the activity of nitrifying bacteria which can destroy the balance of nitration. In this case, the alkaline water or the acid water will retard the nitrification (Qiu et al. 1997). The pH of groundwater in study area ranges from 8.34 to 9.62 which is far beyond the optimal pH for microbiological nitrification. Meanwhile, the most suitable ORP of nitrification is higher than 250 mV. However, the ORP of groundwater in study area is 20 ~ 150 mV. To sum up, it can be determined that the nitrate of groundwater is not formed by microbiological nitrification in the study area.

Conclusions

In this study, we explored the hydrochemical characteristics and enrichment of nitrogen in groundwater in the Tu-Ha area by using the hydrochemical, hydrogen, oxygen, and nitrogen stable isotopes methods. The following conclusions could be drawn:

In the Hami area, the main recharge source of groundwater is from atmospheric precipitation and the groundwater has experienced strong evaporation in study area. The hydrochemistry type is gradually from Cl·SO_4–Na to Cl–Na along the groundwater flow direction, and the concentration change of nitrate, nitrite, ammonia is consistent with that of TDS.

The formation of high level nitrogen in groundwater is consistent to that of Cl^-, Na^+, and SO_4^{2-}, which is mainly affected by strong evaporation. There is no obvious transformation between nitrate, nitrite, and ammonia of groundwater in the study area. The NO_3^-–N/Cl^- ratio of most of samples ranges from 0.02 to 0.05, indicating that the nitrate of groundwater samples in the study area is mainly from natural sources (atmospheric sedimentation), not from the non–Natural sources produced by human activities.

The $\delta^{15}N\text{–}NO_3^-$ ranges from −0.6 to +31 ‰ and mainly in a range of +4.1 to +19.3 ‰, the $\delta^{18}O\text{–}NO_3^-$ ranges from +16.3 to +37.4 ‰. The $\delta^{15}N\text{–}NO_3^-$ and $\delta^{18}O\text{–}NO_3^-$ of most groundwater samples are within the range of atmospheric precipitation. The source of nitrate could be inferred mainly from atmospheric precipitation, and the nitrate in groundwater is not formed by denitrification or microbiological nitrification in the study area.

References

Andersson KK, Hooper AB (1983) O_2 and H_2O are each the source of one O in NO_2 produced from NH_3 by Nitrosomonas: ^{15}N-NMR evidence. FEBS Lett 164:236–240. doi:10.1016/0014-5793(83)80292-0

Aravena R, Robertson WD (1998) Use of multiple isotope tracers to evaluate denitrifi-cation in ground water: study of nitrate from a large-flux septic system plume. Ground Water 36:975–982. doi:10.1111/j.1745-6584.1998.tb02104.x

Barnes CJ, Jacobson Q, Smith GD (1992) Origin of high-nitrate groundwater in the Australian arid zone. J Hydrol 137:181–197. doi:10.1016/0022-1694(92)90055-Z

Böttcher J, Strebel O, Voerkeliust S (1990) Using isotope fractionation of nitrate-nitrogen and nitrate-oxygen for evaluation of microbial denitrification in a sandy aquifer. J Hydrol 114:413–424. doi:10.1016/0022-1694(90)90068-9

Canter LW (1997) Nitrates in groundwater. CRC Press, BocaRaton

Chen JY, Tang CY, Yu JJ (2006) Use of 18O, 2H and 15N to identify nitrate contamination of groundwater in a wastewater irrigated field near the city of Shijiazhuang, China. Journal of Hydrology 326(1/4):367–378. doi:10.1016/j.jhydrol.2005.11.007

Choi WJ, Lee SM, Ro HM (2003) Evaluation of contamination sources of ground water NO_3 using nitrogen isotope data: a review. Geosci J 7:81–87. doi:10.1007/BF02910268

Clark ID, Fritz P (1997) Environmental isotopes in hydrogeology. Fla Lewis Publishers, Boca Raton

Dang YX, Pan KY, Liu ZQ (2010) The basic characteristics and metallogenic mechanism of nitrate mine in Xinjiang. Xinjiang Non ferrous Metal 5:1–5 **(in Chinese)**

Deng L, Cao YQ, Wang WK (2007) An overview of the study on Nitrogen and Oxygen isotopes of Nitrate in groundwater. Adv Earth Sci 22:716–719

Durka W, Schuize ED, Gebauer Q, Voerkelius S (1994) Effects of forest decline and leaching of deposited nitrate determined from ^{15}N and ^{18}O measurements. Nature 372:765–767. doi:10.1038/372765a0

Faillat JP, Rambaud A (1991) Deforestation and leaching of nitrogen as nitrates in underground water in intertropical zones: the example of Cote d'lvoire. Environ Geol Water Sci 17:133–140. doi:10.1007/BF01701569

Friedman I, Machta L, Soller R (1962) Water vapour exchange between a water droplet and its environment. J Geophys Res 67:2761–2766. doi:10.1029/JZ067i007p02761

Galloway JN, Aber JD, Erisman JW (2003) The nitrogen cascade. Bioscience 53(4):341–356

Gates JB, BÖHLKE JK (2008) Ecohydrological factors affecting nitrate Concentrations in a phreatic desert aquifer in northwestern China. Environ. Environ Sci Technol. 42(10):3531–3537. doi:10.1021/es702478d

Gates JB, Edmunds WM, Ma J, Scanlon BR (2008) Estimating groundwater recharge in a cold desert environment in northern China using chloride. Hydrogeol J 16:893–910. doi:10.1007/s10040-007-0264-z

Ge WS, Michalski G, Cai KQ, Wang F, Liu YR (2014) The characteristics and genesis of the massive nitrate deposits in the Turpan-Hami basin of Xinjiang, China. Acta Geologica Sin (Eng Edn) 88(supp. 1):218–219. doi:10.1111/1755-6724.12269_9

Geoffrey T, Dimitri V, Zheng CM (2004) AqQA: quality assurance and presentation graphics for ground water analyses. Ground Water 42(3):326–328. doi:10.1111/j.1745-6584.2004.tb02680.x

Guo YH, Li NN, Zhou ZC et al (2014) Groundwater chemical characteristics in Yamansu and Tianhu section for high level radioactive waste disposal repository. J Nucl Radiochem 36:78–84 **(in Chinese)**

Guo YH, Li NN, Zhou ZC et al (2016) Characteristics and implications of groundwater isotopes in Yamansu and Tianhu preselected section for China's high level radioactive waste disposal repository. Acta Geol Sinica 90(2):376–382 **(in Chinese)**

Hasanah L, Iryanti M, Ardhi ND (2013) Development of software for making contour plot using matlab to be used for teaching purpose. Appl Phys Res. doi:10.5539/apr.v5n1p78

Heaton THE (1990) $^{15}N/^{14}N$ ratios of NOx from vehicle engines and coal-fi red power stations. Tellus 42(3):304–307. doi:10.1034/j.1600-0889.1990.t01-1-00009.x

Hejabi AT, Basavarajappa HT, Karbassi AR, Monavari SM (2011) Heavy metal pollution in water and sediments in the Kabini River, Karnataka, India. Environ Monit Assess 182:1–13. doi:10.1007/s10661-010-1854-0

Hollocher TC (1984) Source of the oxygen atoms of nitrate in the oxidation of nitrite by nitrobacter agilis and evidence against a P-O-N anhydride mechanism in oxidative phosphorylation. Archive Biochem Biophys 233:721–727. doi:10.1016/0003-9861(84)90499-5

Huang TD (2005) Formation of wuyongblake salt lake in Xinjiang and characteristic of potassium nitrate deposit. Xinjiang Geol 23(1):36–40 **(in Chinese)**

Kendall C (1998) Tracing Nitrogen Sources and Cycling in Catchments. In: Kendall C, McDonnell JJ (eds) Isotope Tracers in Catchment Hydrology. Elsevier, Amsterdam, pp 519–576. doi:10.1016/B978-0-444-81546-0.50023-9

Kendall C, Aravena R (2000) Nitrate isotopes in groundwater systems. Environl Tracers Subsurf Hydrol. doi:10.1007/978-1-4615-4557-6_9

Kendall C, McDonnell JJ (1998) Isotope tracers in catchment hydrology. Elsevier, Philadelphia, pp 519–569

Kendall C, Silva SR, Stober QJ (1998) Mapping spatial variability un marsh redox conditions in the Florida ever glade using biomass stable isotopic compositions. EOS 79:s88

Knobeloch L, Salna B, Hogan A (2000) Blue babies and nitrate-contaminated well water. Environ Health Perspet 108(7):675–678. doi:10.2307/3434890

Lee KS, Bong YS, Lee D, Kim K, Kim K (2008) Tracing the sources of nitrate in the Han River watershed in Korea, using δ ^{15}N–NO_3^- and δ ^{18}O–NO_3^- values. Sci Total Environ 2:117–124. doi:10.1016/j.scitotenv.2008.01.058

Li JB (2014) Reviews on study methods of groundwater recharge in arid and semi-arid region. Dissertation, Institute of Geology, China Earthquake Administration, Beijing

Li YH, Qin Y, Liu F (2010) Discovery of mass independent oxygen isotopic compositions in super-scale nitrate mineral deposits from Turpan-Hami Basin, Xinjiang, China and its significance. Geochmica Et Cosmochimica Acta 84(6):1514–1519. doi:10.1111/j.1755-6724.2010.00210.x

Li P, Qian H, Wu J (2014) Origin and assessment of groundwater pollution and associated health risk: a case study in an industrial park, northwest China. Environ Geochem Health 36(4):693–712. doi:10.1007/s10653-013-9590-3)

Li P, Qian H, Howard KWF, Wu J (2015) Building a new and sustainable ''Silk Road economic belt''. Environ Earth Sci 74:7267–7270. doi:10.1007/s12665-015-4739-2

Li P, Wu J, Qian H, Zhang Y, Yang N, Jing L, Yu P (2016) Hydrogeochemical characterization of groundwater in and around a wastewater irrigated forest in the southeastern edge of the Tengger Desert. Expo Health, Northwest China. doi:10.1007/s12403-016-0193-y

Ma J, Edmunds WM (2006) Groundwater and lake evolution in the Badain Jaran desert ecosystem, Inner Mongolia. Hydrogeol J 14(7):1231–1243. doi:10.1007/s10040-006-0045-0

Ma J, Edmunds WM, He J, Jia B (2009) A 2000 year geochemical record of palaeoclimate and hydrology derived from dune sand moisture. Palaeogeogr Palaeoclimatol Palaeoecol 276:38–46. doi:10.1016/j.palaeo.2009.02.028

Mahvi AH, Nouri J, Babaei AA, Nabizadeh R (2005) Agricultural activities impact on groundwater nitrate pollution. Int J Environ Sci Technol 2(1):41–47. doi:10.1007/BF03325856

Mariotti A, Germon JC, Hubert P (1981) Experimental determination of nitrogen kinetic isotope fractionation: some principles; illustration for the denitriflcation and nitrification processes. Plant Soil 62(3):413–430. doi:10.1007/BF02374138

Marret DJ, Khattak RA, Elseewi AA, Page AL (1990) Elevated nitrate levels in soil of eastern of Mojave desert. J Environ Qual 19:658–663. doi:10.2134/jeq1990.00472425001900040005x

Mattern S, Sebilo M, Vanclooster M (2011) Identification of the nitrate contamination sources of the Brusselian sands groundwater body (Belgium) using a dual-isotope approach. Isot Environ Health Stud 3:279–315. doi:10.1080/10256016.2011.604127

McKeon CA, Jordan FL, Glenn EP (2005) Rapid nitrate loss from a contaminated desert soil. J Arid Environ 61:119–136. doi:10.1016/j.jaridenv.2004.08.006

Pan WY (2014) NO_3^- circulation in vadose zone and its response to paleao-hydrology and environment e of Badain Jaran. Dissertation, Lanzhou University

Qin Y, Li YH, Liu F, Hou KJ, Wan DF (2008) Mass Independent Oxygen Isotope Fractionation in Nitrate Deposits of the Turpan-Hami Area, Xinjiang. Acta Geoscientica Sinica 6:729–734

Qin Y, Li YH, Bao HM, Liu F et al (2012a) Massive atmospheric nitrate accumulation in a continental interior desert, northwestern China. Geology 40(7):623–626. doi:10.1130/G32953.1

Qin Y, Li YH, Liu F et al (2012b) N and O isotopes and the ore-forming mechanism of nitrate deposits in the Turpan-Hami Basin, Xinjiang, China. Sci China Earth Sci 55:213–220. doi:10.1007/s11430-011-4358-z

Qiu HX, Liu GQ, Jiao CY (1997) The circulation of nitrogen and groundwater pollution in Xindian area: case study. J Ocean Univ Qingdao 27(4):533–538 **(in Chinese)**

Schaeffer SM, Billings SA, Evans RD (2003) Responses of soil nitrogen dynamics in a Mojave Desert ecosystem to manipulations in soil carbon and nitrogen availability. Oecologia 134:547–553. doi:10.1007/s00442-002-1130-2

Seifert E (2014) OriginPro 9.1: scientific data analysis and graphing software—software review. J Chem Inf Model 54(5):1552. doi:10.1021/ci500161d

Seiler RL (2005) Combined use of ^{15}N and ^{18}O of nitrate and 11B to evaluate nitrate contamination in groundwater. Appl Geochem 20(9):1626–1636. doi:10.1016/j.apgeochem.2005.04.007

Smith SD, Huxman T, Ziter SF (2000) Elevated CO_2 increase productivity and invasive species success in an arid ecosystem. Nature 408:79–82. doi:10.1038/35040544

Umezawa Y, Hosono T, Onodera S, Siringan F et al (2008) Sources of nitrate and ammonium contamination in groundwater under developing Asian megacities. Sci Total Environ 404(2–3):361–376. doi:10.1016/j.scitotenv.2008.04.021

Walvoord MA, Phillips FM, Stonestrom DA (2003) A reservoir of Nitrate Beneath Desert Soils. Science 302(5647):1021–1024. doi:10.1126/science.1086435

Wang DS (1997) Basis for the use of nitrogen isotopes to identify nitrogen contamination of groundwater. Acta Geosicientia Sin 18:221–223 **(in Chinese)**

Weyer P, Cerhan JR, Kross BC et al (2001) Unicipal drinking water nitrate level and cancer risk in older women: tiie Iowa women's health study. Epidemiology 12(3):327–338. doi:10.1097/00001648-200105000-00013

Widory D, Petelet-Giraud E, Negrel P et al (2005) Tracking the sources of nitrate in groundwater using coupled nitrogen and boron isotopes: a synthesis. Environ Sci Technol 39(2):539–548. doi:10.1021/es0493897

Wigand C, McKinney RA, Cole ML, Thursby GB et al (2007) Varying Stable Nitrogen Isotope Ratios of Different Coastal Marsh Plants and Their Relationships with Wastewater Nitrogen and Land Use in New England, USA. Environ Monit Assess 1:71–81. doi:10.1007/s10661-006-9457-5